
SEETHRUFINGER: SEE AND GRASP ANYTHING WITH A MULTI-MODAL SOFT TOUCH

A PREPRINT

Fang Wan

School of Design
Southern University of Science and Technology
Shenzhen, China 518055
wanf@sustech.edu.cn

Zheng Wang

Department of Mechanical and Energy Engineering
Southern University of Science and Technology
Shenzhen, China 518055

Wei Zhang

School of System Design and Intelligent Manufacturing
Southern University of Science and Technology
Shenzhen, China 518055

Chaoyang Song*

Design and Learning Research Group
Southern University of Science and Technology
Shenzhen, China 518055
songcy@ieee.org

September 23, 2024

ABSTRACT

We present SeeThruFinger, a Vision-Based Tactile Sensing (VBTS) architecture using a markerless See-Thru-Network. It achieves simultaneous visual perception and tactile sensing while providing omni-directional, adaptive grasping for manipulation. Multi-modal perception of intrinsic and extrinsic interactions is critical in building intelligent robots that learn. Instead of adding various sensors for different modalities, a preferred solution is to integrate them into one elegant and coherent design, which is a challenging task. This study leverages the in-finger vision to inpaint occluded regions of the external environment, achieving coherent scene reconstruction for visual perception. By tracking real-time segmentation of the Soft Polyhedral Network's large-scale deformation, we achieved real-time markerless tactile sensing of 6D forces and torques. We demonstrate the capable performances of the SeeThruFinger for reactive grasping without using external cameras or dedicated force and torque sensors on the fingertips. Using the inpainted scene and the deformation mask, we further demonstrate the multi-modal performance of the SeeThruFinger architecture to simultaneously achieve various capabilities, including but not limited to scene inpainting, object detection, depth sensing, scene segmentation, masked deformation tracking, 6D force-and-torque sensing, and contact event detection, all within a single input from the in-finger vision of the See-Thru-Network in a markerless way. All codes are available at <https://github.com/ancorasir/SeeThruFinger>.

Keywords In-finger Vision · Multi-Modal Perception · Segmentation Tracking · Scene Inpainting

1 Introduction

Vision-based sensing is probably the most widely adopted perceptual modality in modern robotics, transforming the unstructured environment into a structured embodiment for reasoning and learning in an object-centric manner [1]. Besides bioinspiration from the human's hand-eye system, robotic vision provides a unified representation of the 3D world into matrices of 2D pixels that have evolved rapidly in both theoretical foundations and engineering applications, which is further accelerated by recent advancements in data science and deep learning [2]. While the classical methods focus on the visual features to extract reusable information analytically [3], recent development exploits data-driven

*Corresponding Author.

methods by systematically integrating promptable segmentation tasks, pre-trained foundation models, and web-scale datasets to segment anything [4]. Such capability provides researchers with further insights to achieve object tracking [5], object classification [6], pose estimation [7], occlusion inpainting [8], and scene reconstruction [9] with pixel-level details in an automatic workflow, paving the path towards a multi-modal physical embodiment of machine intelligence for robot learning [10]. It should be noted that vision-based perception remains a leading choice for many robot learning research and applications despite the growing accessibility and availability of other perceptual modalities.

Due to basic principles such as line-of-sight, ambient lighting, and surface reflection, problems such as occlusion remain challenging in robotic vision. Occlusion is a practical problem caused by optical physics, which is inevitable for robot workstations that mainly adopt cameras as the only or primary sensor for extrinsic perception. To perform iterative visual verification during object manipulation [11], researchers usually need to add more cameras [12] or move the gripper to a particular pose to expose the fingers in the viewing range for grasp result checking. These solutions make trade-offs in hardware, integration, or time cost. While it is always possible to add more sensors or use more powerful ones, it remains a difficult design task to integrate multiple sensory modalities within a compact form factor for robotic manipulation [13].

1.1 Occlusion in Common Hand-Eye Systems

The robotic manipulation problem is typically set up as a Hand-Eye system [14], as illustrated in Fig. 1A. The “Hand” represents a gripper attached to an “Arm” manipulator’s flange for handling physical contact with objects. The “Eye” is an external camera for visual perception. Since only light signals with unobstructed lines of sight could be captured by the camera, occlusions commonly occur when some objects are stacked on the other. For example, Object 1 in Fig. 1A is placed at the top with its complete shape captured in the image, but parts of Objects 2 and 3 are occluded since they are placed underneath. Inspired by the human approach, roboticists have investigated different solutions to address occlusion via better tools, more skills, or multi-modal interactions.

- Human usually adopts the *better-tools* solution by upgrading hardware or software without disrupting the original task pipeline. For example, in many scenarios, the occlusion problem could be partially alleviated by using more capable machine vision systems, such as 3D vision capturing the scene in dense point cloud data [15], or more efficient learning algorithms to handle complexities in feature extraction [16].
- The *more-skills* solution is also a human-inspired strategy, which involves rearranging the scene via added skills in motion planning so that the occluded objects can be visually captured in sufficient detail. Motion planning using convex optimization enables added skills for robotic arms to move around obstacles for object manipulation [17]. Sampling-based planning with hierarchical graphs also provides capabilities to retrieve objects in cluttered scenes by moving obstacles around until the target object is found [18].
- The *multi-modal* solution introduces further perceptual modalities to aid in handling uncertainties caused by occlusions. Tactile sensory from the skin, especially those on the fingertips, is a biological answer to this problem with evolutionary evidence [19]. Introducing tactile sensing on top of robotic vision enhances learning manipulation skills, formulating a coarse-to-fine hierarchy between globalized scene understanding and localized manipulation dynamics [20].

1.2 Vision-based Tactile Sensing Architectures

The robotics research community is interested in Vision-Based Tactile Sensing (VBTS) to complement visual perception through contact [21, 22]. While researchers have developed various tactile sensors utilizing different sensing principles [23, 24], VBTS solutions remain preferred among robotic researchers in academia and applications [25]. Some advantages include easy access to camera sensors, unified data structure, shared theories and learning models from computer vision, and deep learning. However, due to the size of the camera board, the field of view, choice of lenses, and electrical wiring, it remains a design problem for vision-based tactile sensors to be seamlessly compatible with various multi-fingered gripper systems. Recent literature reports several in-depth review articles on the technical specifications and theoretical foundations of VBTS [26]. In the following, we focus our review on the design analysis of two VBTS architectures, one with an Illuminated Chamber in Fig. 1B and another with a See-Thru-Network in Fig. 1C.

In-finger vision represents a general architecture of VBTS, which mainly features an Illuminated Chamber design illustrated in Fig. 1B. A miniature camera is installed within a closed chamber, physically isolated from the ambient environment. Therefore, active lighting using LEDs is usually required to enable the proper functions of the camera [27]. In front of the lens is a soft membrane made from transparent elastomer, covered with a layer of opaque coating on the outer surface, blocking the line of sight. Before contact occurs on the soft membrane’s outer surface, VBTS with an Illuminated Chamber design usually cannot capture visual features of the external environment. Instead, it requires

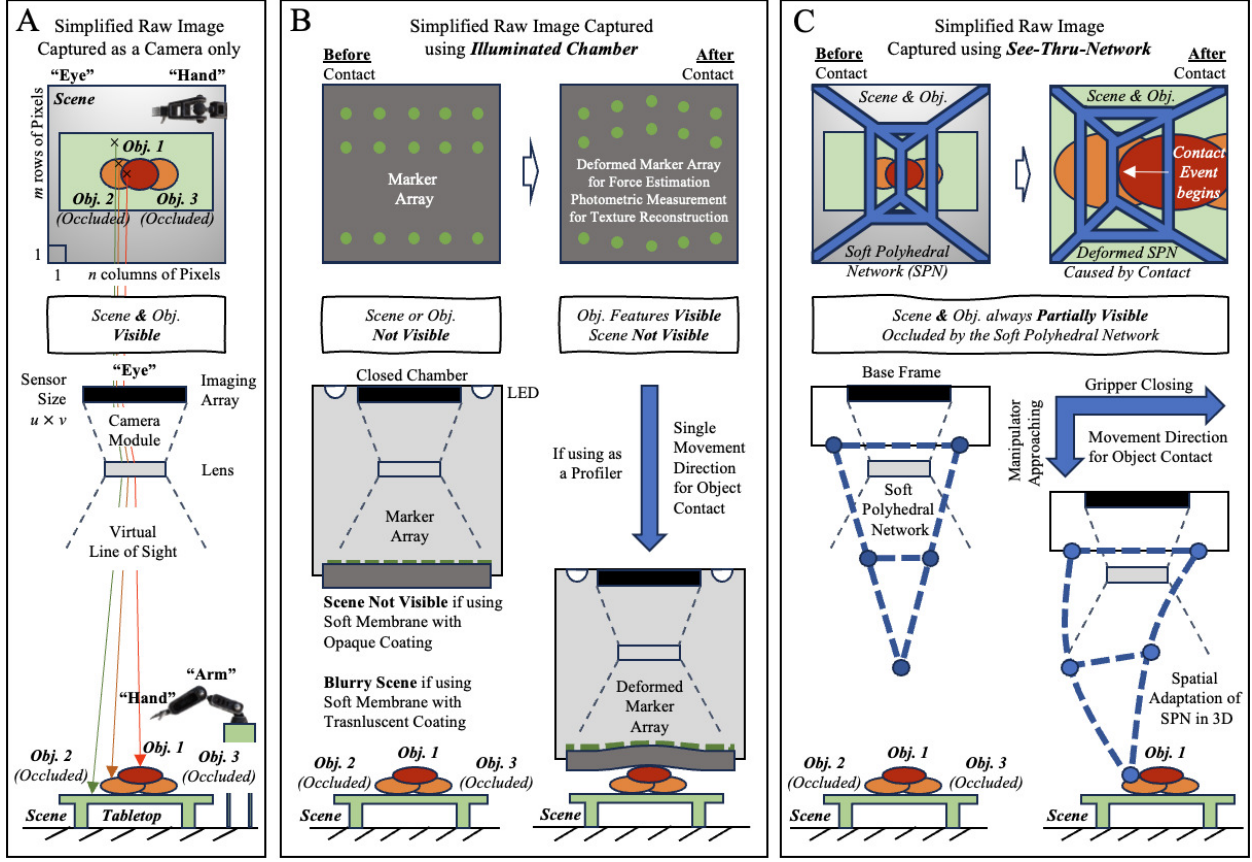


Figure 1: **Review of Vision-based Tactile Sensing (VBTS) architectures.** (A) A generalized illustration of the visual perception process in a typical “Hand-Eye” system and simplified illustrations of VBTS architecture via (B) an Illuminated Chamber or (C) a See-Thru-Network.

a touch event on the soft membrane to induce imprinted textures, assisted by active lighting in a predefined color sequence inside to enable visual capturing of the refined textures via photometric processing. In addition, researchers usually paint artificial marker arrays on the inner surface of the soft membrane [28] or even directly embed these markers inside [29] to enable estimation of the tactile forces and torques. A representative application of VBTS with an Illuminated Chamber design is as a profiler for surface measurement by moving the sensor directly toward the target surface. However, like human fingers, the robotic finger usually detects tactile interactions on the side of the fingertip when the gripper closes, assisted by the manipulator’s general motion to approach the object, as shown in Fig. 2A.

As a result, researchers usually need to rotate the sensor during implementation, as shown in Fig. 2B, when fixing VBTS with an Illuminated Chamber on the robotic fingertip. Researchers recently explored design modifications by adding a reflective and opaque mirror inside to change the light path, as shown in Fig. 2C(i), so the sensor could be more conveniently fitted on robotic fingertips [30]. Design modification could be done using a translucent coating instead so that partial light from the outside could pass through the soft membrane [31, 32]. This enables visual perception of the scene at a close distance before the contact event, as the image is usually blurry due to the translucent coating used. A similar design modification is to use a reflective in Fig. 2C(i) or a translucent mirror in Fig. 2C(ii) to achieve similar purposes.

Recent research also reports another architecture for VBTS using a See-Thru-Network, as illustrated in Fig. 1C. A Soft Polyhedral Network (SPN) replaces the soft membrane with a hollow space inside to enable a see-through design [33, 34]. The SPN is a soft robotic metamaterial capable of geometric adaptations in omni-directional interactions. One can fix fiducial markers inside the SPN, transforming its spatial adaptations into the marker’s 6D movement, visually tracked by the miniature camera inside. This enables an open base frame, allowing the camera lens to be fully exposed to the external environment [35]. Leveraging the See-Thru-Network design, the images captured contain two layers of information following the line-of-sight principle. The first layer is the structural state of the SPN, followed by a second layer showing a partial view of the scene and objects occluded by the SPN. When adopting a finger-like design for

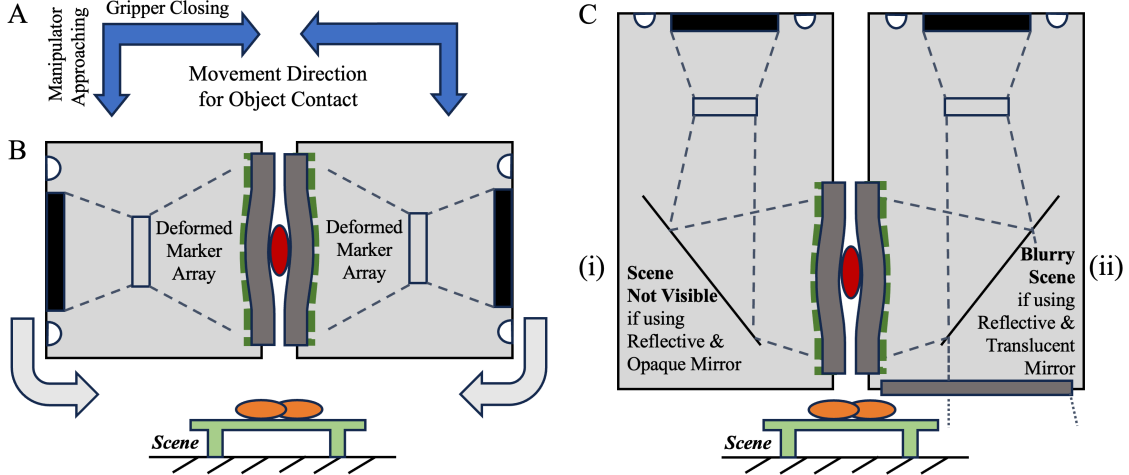


Figure 2: **Practical usage of vision-based tactile sensing using an illuminated chamber.** (A) A combined movement direction with the manipulator approaching the object and the fingers closing for picking. (B) Rotated assembly of the illuminated chambers to facilitate tactile sensing on the finger surface. (C) An alternative approach to changing the light path is using a mirror of different optical features.

the SPN, primary interactions occur on the primary side of the SPN, allowing the whole finger to be installed with the in-finger camera directly facing the scene. As the manipulator approaches the object, an occluded view of the scene and objects is always visible to the in-finger camera but impeded by a fixed image of the SPN. When the gripper closes in a lateral direction until contact begins, the SPN interacts with the object through omni-directional adaptation, fully captured by the in-finger vision.

While both VBTS architectures feature an in-finger vision component, they provide tactile perception at different levels of detail when integrated with a robot manipulation system. Using photometric imaging within an enclosed chamber, the Illuminated Chamber design excels in refined texture reconstruction within a small range of soft membrane deformation. On the other hand, See-Thru-Network provides large-scale geometric adaptation while producing high-performing 6D force and torque estimation that is not limited to common on-land scenarios but applies to the underwater environment [36, 37].

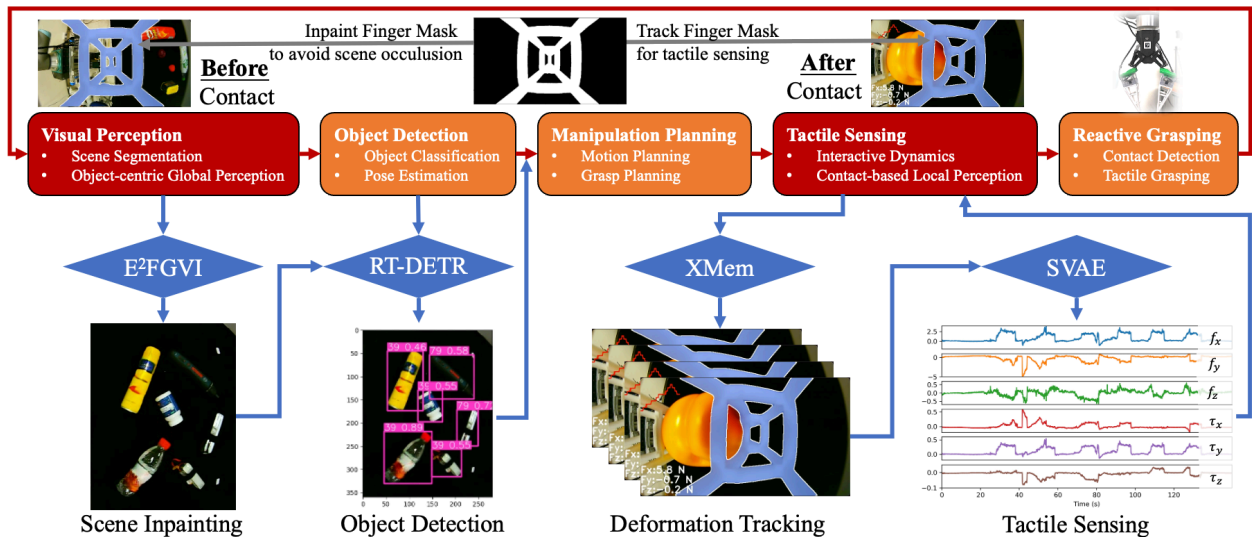


Figure 3: **A basic implementation of Multi-Modal Perceptual Embodiment via the proposed SeeThruFinger architecture, which simultaneously learns visual perception (object detection in this example) and tactile sensing using the in-finger vision of a Soft Polyhedral Network’s See-Thru feature.**

1.3 Proposed Method and List of Contributions

This study proposes the SeeThruFinger architecture, as shown in Fig. 3, using the Soft Polyhedral Network for simultaneous visual perception of the scene and tactile sensing of physical contacts via in-finger vision, achieving markerless Vision-Based Tactile Sensing with a See-Thru-Network. Before the contact begins, a static mask of the SPN is used to inpaint the occluded scene from in-finger vision via a head-up movement. The inpainted in-finger vision reconstructs the scene, enabling typical downstream capabilities such as object detection for grasping. Then, we implement markerless, real-time, and large-scale deformation tracking of the SPN via video object segmentation using the SPN’s static mask. Real-time monitoring of the SPN’s deformation mask enables us to achieve markerless tactile sensing by learning to infer high-performing 6D forces and torques during grasping. Finally, we demonstrate the feasibility of our proposed SeeThruFinger architecture through a reactive grasping task. We also demonstrate SeeThruFinger’s potential in multi-modal perceptual embodiment to simultaneously achieve various downstream capabilities such as object detection, depth sensing, and scene segmentation after scene inpainting, which benefits from the growing adoption of foundational models. Overall, the SeeThruFinger architecture holds the potential to systematically simplify the hardware requirement of a typical Hand-Eye system through multi-modal perceptual fusion using a single in-finger vision sensor. Contributions of this study are listed as follows:

- This study proposes the SeeThruFinger architecture for Vision-based Tactile Sensing (VBTS), achieving simultaneous decoupling of tactile sensing for physical contact and multi-modal visual perception, such as object detection, depth sensing, and scene segmentation, within a single in-finger vision system.
- This study is among the first to achieve markerless VBTS using real-time masked segmentation and scene inpainting by leveraging the See-Thru-Network’s occluded design features for enhanced multi-modal tactile perception.
- This study also validates the proposed method’s competitive performance against traditional hand-eye systems in a multi-object reactive grasping demonstration via a single SeeThruFinger without using external cameras, dedicated tactile sensors, or force-torque sensors.

2 Preliminaries & Problem Formulation

We begin by denoting an image $\mathbf{X}_t \in \mathbb{R}^{m \times n}$ captured by a camera at timestep t . The m and n are the user-defined output settings for the image size, measured in the total count of pixel rows and columns. Depending on the camera selection, the i th row and j th column pixel entry of the image $x_{i,j,c,t}$ may contain the brightness intensity of a single channel for grayscale images ($c = 1$) or three channels in red, green, and blue (RGB) for color images ($c = 1, 2, 3$). Each pixel entry usually stores information in an 8-bit format, offering 256 conditions ranging from 0 to 255. Furthermore, we can add another data channel ($c = 4$) to the RGB image to include each pixel’s transparency state.

2.1 Markerless Design of the SeeThruFinger

Shown in Fig. 4 is the Hand-Eye system adopted in this study, built with aluminum extrusion based on the DeepClaw workstation [14], housing a collaborative robot (UR10e from Universal Robots) on a pedestal and a tabletop in front covered by black fabrics. Although an “Eye” camera is fixed on the post shown in Fig. 4A, it is intentionally unplugged (therefore with a strikethrough) as we intend to implement visual perception of the scene using in-finger vision only from the SeeThruFinger. Figure 4B shows an enlarged view of the “Hand,” a two-fingered gripper (Model AG-160-95 from DH-Robotics) with its fingertips replaced by the SeeThruFingers. Each SeeThruFinger contains a soft, omni-adaptive, markerless finger based on a variant of the Soft Polyhedral Network designs [34], mounted on a camera housing 3D-printed by UV-curable transparent resin (Somos WaterShed XC 1112), where a miniature camera (Chengyue WX605 from Weixinshijie) is fixed inside, as shown in Fig. 4C. One can customize the base plate to install the SeeThruFinger on Force-Torque (FT) sensors for testing or on a gripper as fingertips for soft

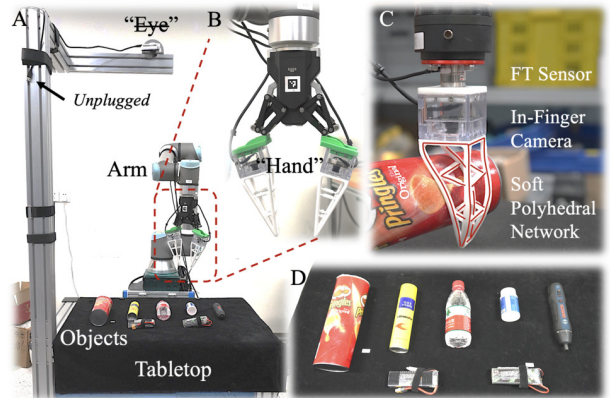


Figure 4: **Experiment setup of a typical Hand-Eye system.** (A) The DeepClaw workstation used in this study with the “Eye” camera intentionally unplugged. (B) Enlarged view of the “Hand” gripper with the SeeThruFingers installed. (C) The markerless SeeThruFinger setup collects training data against FT sensors. (D) The test objects used in this study.

and adaptive grasping. Figure 4D shows the objects used for testing in this study, including a Pringles Can from the Yale-Columbia-Berkley (YCB) object sets [38] and others commonly available at research labs, including spray can, mineral water bottles filled halfway with water, medicine bottle, Bosche electrical screwdriver, pouch cell. Although both SeeThruFingers on the gripper are functional, we only used the one whose viewing range partially covers the table at every frame throughout the following experiments.

2.2 Formalizing Multi-Modal VBTS via a See-Through-Network

For an image $\text{InFinger}\mathbf{X}_t$ taken by an in-finger vision camera, such as the case shown in Fig. 1A, the resultant image is essentially the same as the general representation $\text{InFinger}\mathbf{X}_t = \mathbf{X}_t$ reproduced in Fig. 5. The ambient environment is gray in Fig. 5. If the in-finger camera is used for VBTS architecture with an Illuminated Chamber (IC) shown in Fig. 1B, then any i th row and j th column pixel of the image $\text{IC}x_{i,j,t}$ is regarding the state of the soft membrane captured within the camera’s viewing range, containing zero information about the scene before contact begins.

However, for an image $\text{STN}\mathbf{X}_t$ taken by an in-finger camera for VBTS architecture with a See-Through-Network (STN), such as the case shown in Fig. 1C, the resultant image contains the scene occluded by the Soft Polyhedral Network (SPN). We denote the image as $\text{STN}\mathbf{X}_t = \text{STN}\mathbf{X}_t$ if the SPN is in a Static State before any contact. We can add a hat to use the symbol $\text{STN}\widehat{\mathbf{X}}_{\text{Static}}$ to indicate a particular case if the scene is empty, captured as uniform pixel features. Here, the subscript timestep t is removed to simplify the representation. Since the valuable information captured in this image is purely regarding the SPN, one can add a transparency channel to obtain $\text{STN}\widehat{\mathbf{X}}_{\text{Static}}$, represented in white color in Fig. 5. Pixel data of the SPN is preserved in this added data channel, but the pixel data of the empty scene is set to transparent. Such an operation would produce a matrix $\text{STN}\widehat{\mathbf{M}}_{\text{Static}}$ that can be visualized as a Static Mask of the segmented SPN. Element-wise matrix multiplication of image $\text{STN}\mathbf{X}_t$ and this Static Mask will produce masked image $\text{STN}\mathbf{X}_t^{\text{Masked}}$. Note that performing the same operation using raw image $\text{InFinger}\mathbf{X}_t$ will produce the same masked image instead. This also explains the SPN’s See-Through feature in the in-finger vision image occlusion process. The above process generally applies to scenarios when the SPN is in a Static State, meaning that no deformation is induced as there is no contact event. One can use classical image processing techniques to obtain the above results.

However, the above process becomes complicated when contact events occur at $t = \text{Contact}$. On one side, the SPN enters a Dynamic State, exhibiting whole-body adaptive deformation during physical contact with the objects. On the other side, the See-Through scene also changes during contact, adding to the complexity of segmentation. The resultant image $\text{STN}\mathbf{X}_t$ captured by the in-finger camera can be represented as $\text{STN}\mathbf{X}_{t=\text{Contact}}$ when contact begins. Let us assume that the Dynamic Mask of the segmented SPN, $\text{STN}\mathbf{M}_{t=\text{Contact}}^{\text{Seg}}$, could be obtained. Then, one should be able

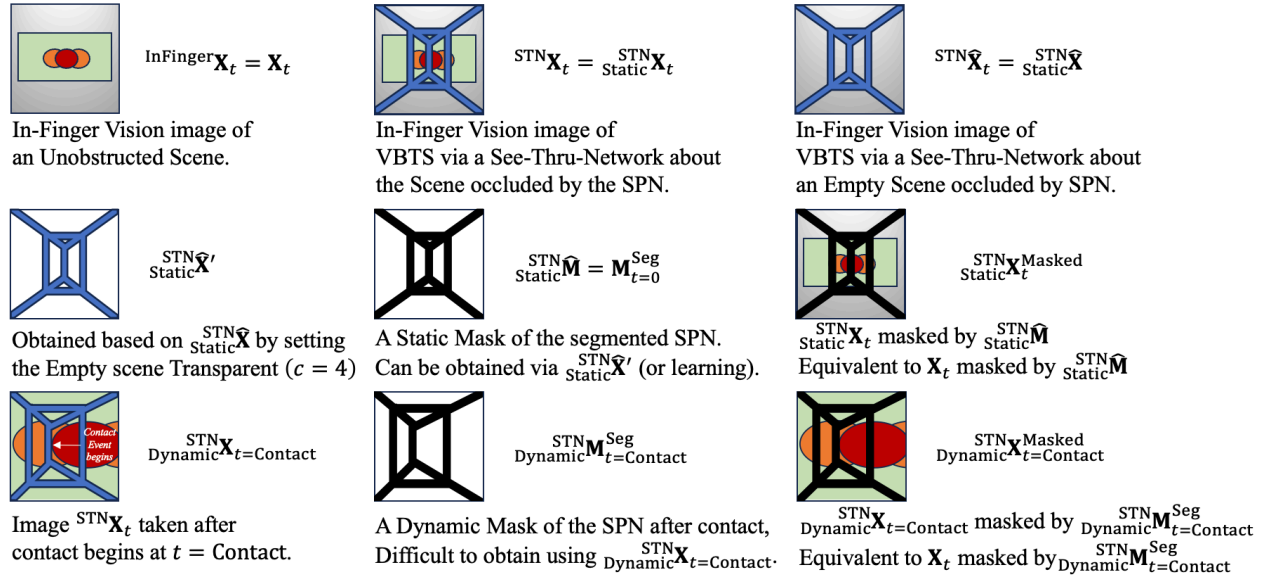


Figure 5: Illustrations of the image processing pipeline for VBTS architecture via See-Through-Network when using classical machine vision techniques.

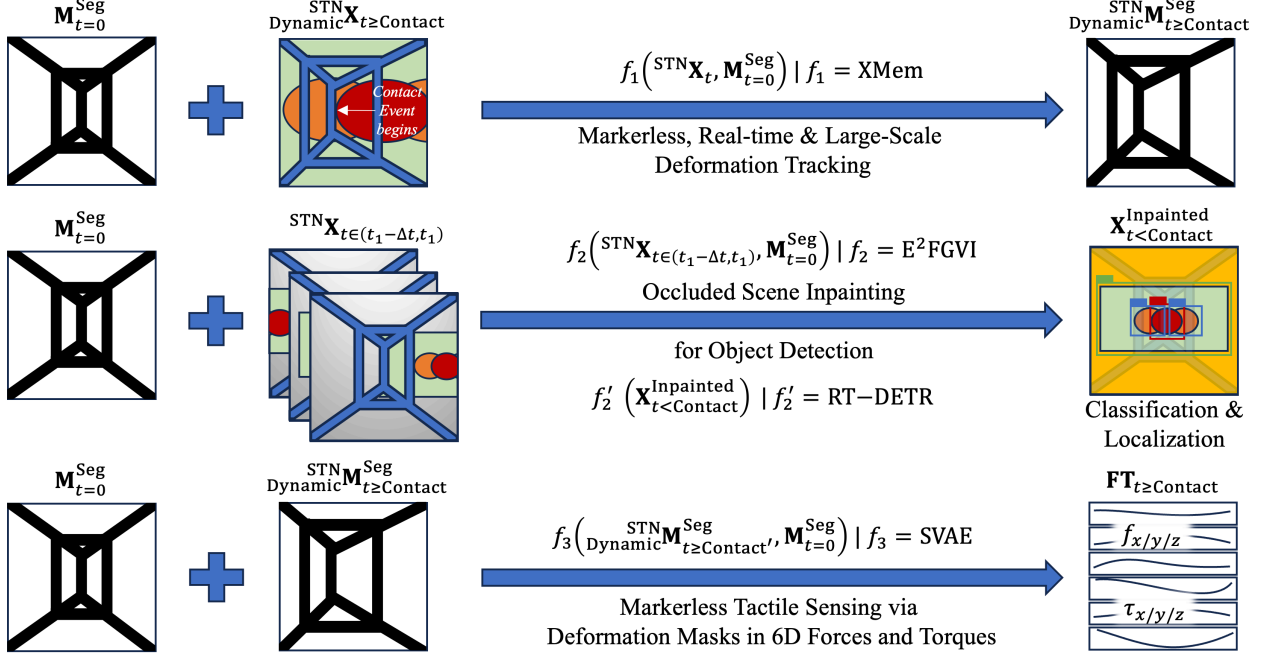


Figure 6: Formalization of the three research problems for VBTS architecture via a See-Thru-Network.

to obtain a masked image of the in-finger vision, $\text{Dynamic}_{t=\text{Contact}}^{\text{STN}} \mathbf{X}_{t=\text{Contact}}^{\text{Masked}}$, by performing the same pixel-wise multiplication of $\text{Dynamic}_{t=\text{Contact}}^{\text{STN}} \mathbf{X}_{t=\text{Contact}}^{\text{Masked}}$ using this Dynamic Mask. Similarly, this would be equivalent to applying the Dynamic Mask over an unobstructed in-finger vision image $\text{InFinger} \mathbf{X}_t$. The challenge is that such a Dynamic Mask of the SPN will be intricate to obtain using classical methods, especially in cluttered scenes, which usually require advanced segmentation processing and feature engineering.

Using the symbols above, we formalize three research problems of this study for a generic scenario of reactive object grasping where both 1) scene-wise visual perception for object detection and 2) object-centric tactile sensing for force-and-torque sensing are considered.

1. Throughout the whole grasping process, can we perform markerless, real-time, and large-scale deformation tracking of the interactive medium, i.e., the Soft Polyhedral Network, in both Static and Dynamic States to obtain a pixel-wise mask $\mathbf{M}_t^{\text{Seg}}$?
2. Before contact begins, can we reconstruct the unobstructed scene $\mathbf{X}_{t < \text{Contact}}$ from occluded in-finger images $\text{STN} \mathbf{X}_{t < \text{Contact}}$ for visual perception, i.e., object detection, in a Hand-Eye system via in-finger vision only?
3. During contact-based physical interactions, can we infer high-precision tactile sensing of 6D forces and torques $\mathbf{FT}_{t \geq \text{Contact}}$ in a markerless way?

Figure 6 illustrates these three research problems when applying the soft polyhedral networks with in-finger vision as the fingertips. The following section will provide further details on addressing these three research problems by leveraging state-of-the-art algorithms from computer vision. Section 4 offers a full experimental demonstration of reactive grasping using the SeeThruFingers only. All three research problems are addressed using the See-Thru-Network architecture without external cameras or dedicated force-and-torque sensors. Section 5 discusses the further expansion of these three research problems into a multi-modal approach for robotics using vision-based tactile sensing via SeeThruFingers.

3 Methods & Results

3.1 Markerless, Real-time, Large-Scale Deformation Tracking

The first problem is to enable markerless real-time segmentation tracking of the SPN’s adaptive deformation during contact, which always covers a considerable amount of the image area with large-scale spatial deformations. This problem is equivalent to video object segmentation in computer vision. A significant challenge of this problem is

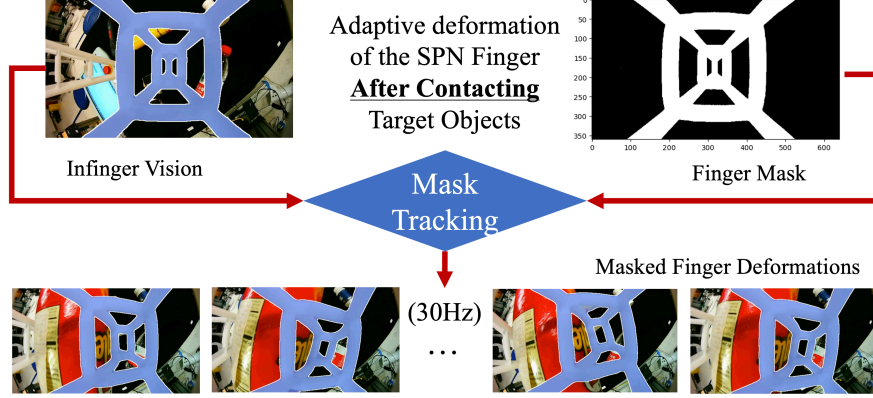


Figure 7: **Markerless deformation tracking of the Soft Polyhedral Network (SPN) mask.**

to efficiently manage the feature memory model to avoid memory explosion with minimized performance decay for long-term predictions, where the latest development in a Unified Memory architecture, the XMem model, exhibits state-of-the-art performances on long-video benchmarking datasets [5].

In this study, we experimented with the XMem model for the in-finger video stream, as shown in Fig. 7, achieving a real-time implementation (30 Hz) of the SPN’s large-scale deformation mask in a markerless way. This is realized by using a Static Mask of the SPN $\widehat{\mathbf{M}}_{\text{Static}}^{\text{STN}}$ as the initial tracking target and the in-finger vision image $\mathbf{X}_{t \geq \text{Contact}}^{\text{STN}}$ of the SPN after contact. Before any contact event, this Static Mask remains the same and can be conveniently obtained manually or using advanced segmentation algorithms such as SAM [4].

We evaluated this mask segmentation over a test dataset of 1,000 samples with the ground truth masks. The region (J) and boundary (F) measures [39] are 0.975 and 0.997, respectively, showing excellent reliability in tracking the soft finger’s spatial deformation masks in a markerless way. In applications, we found that the XMem’s mask tracking of the SPN’s deformation is not limited to the Dynamic States but also applicable to the Static States of the SPN. We successfully implemented markerless and real-time deformation tracking of the SPN whenever the SeeThruFinger architecture is enabled, alleviating the need for artificial markers reported in previous VBTS literature. In other words, this process can be alternatively used to detect the occurrence of a contact event. This leads to the formal representation of this implementation as the following, addressing the first research problem in Fig. 6.

$$\begin{aligned} \text{STN} \mathbf{M}_t^{\text{Seg}} &= f_1(\text{STN} \mathbf{X}_t, \mathbf{M}_{t=0}^{\text{Seg}}), \\ f_1 &= \text{XMem}. \end{aligned} \tag{1}$$

3.2 In-Finger Visual Perception from Scene Inpainting

The second problem is reconstructing the scene using occluded images captured by the in-finger vision for visual perception, such as object detection, providing the equivalent capability to an external “Eye” camera. Due to the SPN’s See-Through feature, this problem becomes comparable to the classical inpainting problem, a conservation technique to fill in damaged, deteriorated, or missing parts of an artwork to present a complete and coherent image. Video inpainting has recently attracted significant interest from the computer vision research community, where learning-based methods exhibit superior performances in filling in missing regions of a video with spatially and temporally coherent contents [40].

Therefore, we propose to move around the SeeThruFinger shown in Fig. 8A to obtain redundant information about the scene by scanning sequential in-finger images from different angles about the same scene, accumulating sufficient visual features from the See-Through pixels to inpaint the occluded scene. Figure 8B illustrates a hard-coded head-up movement of the gripper for the in-finger camera to capture a short video $\text{STN} \mathbf{X}_{t \in (t_1 - \Delta t, t_1)}$ in which its viewing range sweeps across the tabletop scene. The predefined movement can also be set to linear movement above the robot’s working area with a fixed orientation. The first row of Fig. 8C shows the in-finger vision of the scene without attaching the SPN on the SeeThruFingers, the second row with the soft finger occluding the scene, and the third row for the corresponding frames of the inpainted scene. Only the right half of the image with objects is inpainted for efficient processing. We ensured that all objects have been captured in at least one or more frames in the video, providing context for reconstructing frames where SPN blocks objects.

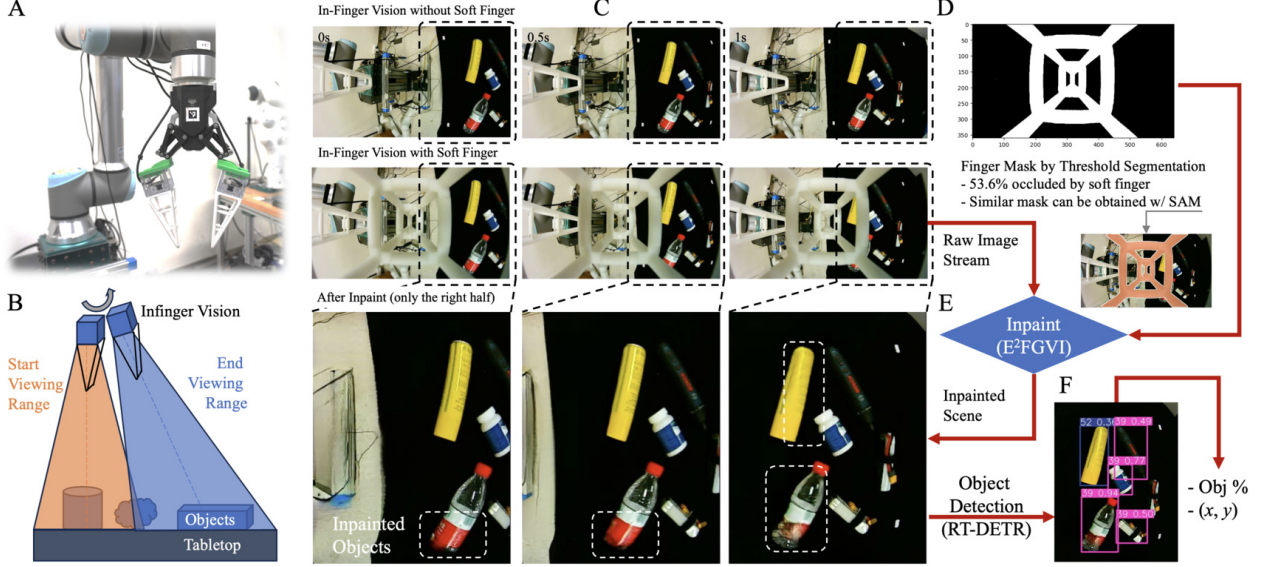


Figure 8: **The method of in-finger visual perception from occluded scene inpainting using VBTS architecture via a See-Thru-Network.** (A) SeeThruFingers attached to the fingertips of Model AG-160-95 gripper from DH-Robotics. (B) Illustration of the scene scanning process by slightly tilting the gripper above the tabletop for a short ($\Delta t \approx 1$ sec) video clip for inpainting. (C) Selected images at 0 sec, 0.5 sec, and 1 sec from the head-up motion video clip without the soft finger, with the soft finger, and after inpainting in each row. (D) A Static Mask of the SPN obtained by threshold segmentation. (E) The inpainting operation. (F) Visual perception of the inpainted scene for object detection, including object classification and localization.

Then, we implemented the End-to-End framework for the Flow-Guided Video Inpainting (E^2FGVI) algorithm [41], a state-of-the-art algorithm for video inpainting. To facilitate the inpainting process, we obtain a Static Mask of the SPN in Fig. 8D using threshold segmentation against a clean background, denoted as $\widehat{M}_{Static}^{STN}$. Results show that the SPN occludes about 53.6% of the in-finger image pixels. Alternatively, we can interactively obtain the same mask using the Segment Anything Model (SAM) by clicking for comparison in an actual scene [4]. Visual perception is usually performed before the contact event when $0 \leq t < \text{Contact}$ for an object manipulation pipeline. During this period, the SPN is in a Static State, meaning that the resultant mask remains unchanged as the initial mask $M_{t=0}^{Seg} = \widehat{M}_{Static}^{STN}$. The E^2FGVI algorithm has been reported with a high Structural Similarity Index (SSI) measure of 0.97 on two public datasets, YouTube-VOS and DAVIS, under stationary masks.

Figure 8E shows the scene inpainting pipeline to implement the E^2FGVI algorithm using in-finger video clip $\widehat{X}_{t \in (t_1 - \Delta t, t_1)}^{STN}$ and the SPN's Static Mask $M_{t=0}^{Seg}$ to generate inpainted scene $\widehat{X}_{t < \text{Contact}}^{Inpainted}$ with objects on the tabletop. This inpainting process is represented as

$$\begin{aligned} \widehat{X}_{t < \text{Contact}}^{Inpainted} &= f_2(\widehat{X}_{t \in (t_1 - \Delta t, t_1)}^{STN}, M_{t=0}^{Seg}), \\ f_2 &= E^2FGVI \end{aligned} \quad (2)$$

The inpainted images managed to reconstruct sufficient details of the occluded objects and the scene, as shown in the dashed white boxes in Fig. 8C.

We further implemented a variety of visual perception tasks based on the inpainted scene to demonstrate the feasibility of in-finger visual perception. Firstly, we use the Real-Time DEtection TRansformer (RT-DETR), a state-of-the-art object detection algorithm [42]. This object detection process is represented as

$$\begin{aligned} \{\%, (x, y)\} &= f'_2(\widehat{X}_{t < \text{Contact}}^{Inpainted}), \\ f'_2 &= \text{RT-DETR}. \end{aligned} \quad (3)$$

The example shown in Fig. 8F verifies the feasibility of visual perception using an inpainted scene from in-finger vision occluded by the SPN, producing object classification (%) and bounding box center (x, y) that can be later used for motion planning. Equations (2) and (3) are the formal representation of this implementation, addressing the second research problem in Fig. 6.

3.3 Markerless Tactile Sensing via Deformation Mask

The third problem is to infer high-performing tactile sensing in a markerless way using in-finger vision of the SPN. This representation problem is usually resolved by adding artificial markers to the soft medium during physical interactions, which VBTS architectures share using either an Illuminated Chamber or a See-Thru-Network. Previous research also explored fiducial markers inside the SPN, achieving high-performing tactile sensing, especially when considering the SPN’s static and dynamic viscoelasticity [33].

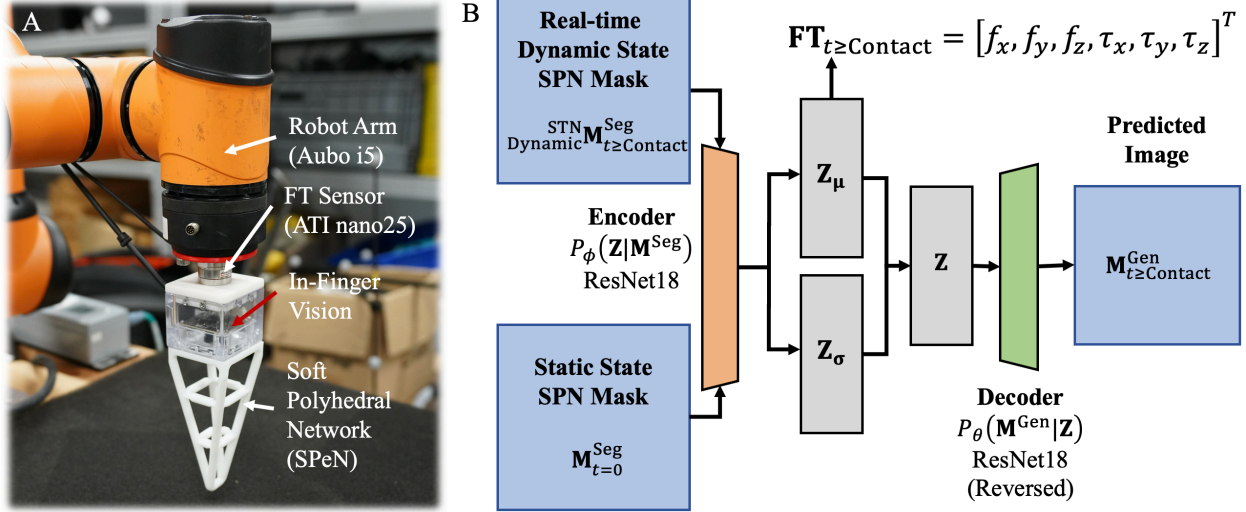


Figure 9: **Experimental setup and the Supervised Variational Autoencoder model for tactile sensing.** (A) Experiment setup for collecting training data. (B) Supervised learning framework for 6D force/torque prediction.

This study uses the SPN masks in the Dynamic States obtained from segmented tracking as the model input to infer tactile sensing in 6D forces and torques. We adopted the Supervised Variational AutoEncoder (SVAE) for this task, and Fig. 9A shows the experimental setup for collecting true labels of 6D forces and torques at the finger base using nano25 by ATI for calibration. The in-finger camera and FT sensor were connected to a laptop for data streaming. We collected 40,000 synchronized pairs of images and FT readings while manually compressing the two SPN fingers from various directions and contact locations. We used an 8:2 train-valid split and trained the SVAE model for 50 epochs. To avoid excessive good validation scores due to the potential sample dependence, we separately collected a test dataset of 1,000 samples.

Figure 9B illustrates the SVAE model. The SPN masks segmented in Dynamic States $STN_{Dynamic} M_{t \geq Contact}^{Seg}$ and the mask template $M_{t=0}^{Seg}$ are fed to the ResNet18 encoder and decoder module to reconstruct the in-finger image $M_{t \geq Contact}^{Gen}$. The latent space is set to 32-dimension. At the same time, we design an auxiliary supervised regression task of the 6D forces and torques $FT_{t \geq Contact}$ simultaneously from the learned latent geometry representation. This leads to the formal representation of this implementation as the following, addressing the third research problem in Fig. 6.

$$\{FT_{t \geq Contact}, M_{t \geq Contact}^{Gen}\} = f_3(STN_{Dynamic} M_{t \geq Contact}^{Seg}, M_{t=0}^{Seg}), \quad (4)$$

$$f_3 = \text{SVAE}.$$

The overall loss consists of reconstruction loss, the Mean-Squared Errors (MSE) loss of force and torque prediction, and the Kulback-Leibler divergence. The average time for a single inference is 1.9 ms on an NVidia 3080 Ti Laptop GPU. The Mean Absolute Errors of the validation and test dataset are reported in Table 1, indicating good generalization of the learned model.

Table 1: **Evaluation of the Supervised Variational AutoEncoder (SVAE) model for in-finger tactile sensing.**

MAE Datasets	Force (N)			Torque (Nm)		
	f_x	f_y	f_z	τ_x	τ_y	τ_z
Validation dataset	0.241	0.212	0.14	0.024	0.027	0.005
Test dataset	0.328	0.283	0.24	0.027	0.036	0.005

Figure 10A compares the test dataset’s prediction and ground truth in time series. Figure 10B shows the scatter plot of such comparison in the validation dataset with excellent R^2 scores over 0.985 in all components except f_z . The relatively weak performance in f_z is due to the limited adaptability along the z -axis. We also evaluate the resultant force in the xy plane and find the mean magnitude and orientation error are 0.286 N and 2.6 degrees, respectively.

4 Reactive Grasping with SeeThruFingers

This section demonstrates the application of the proposed SeeThruFinger architecture, shown in Fig. 3, in an object-picking task, shown in Fig. 4, using VBTS with a SeeThru-Network to achieve object detection and tactile sensing for reactive grasping simultaneously.

The task begins with visual perception of the scene using the SeeThruFinger for object classification and localization. During the first attempt, the gripper will attempt to pick up the object at the center of the bounding box and a fixed rotation angle θ_0 and depth z_0 perpendicular to the table. We intentionally used a simpler algorithm without the optimal orientation to test reactive grasping with tactile sensing using the SeeThruFinger. In our previous work [43], it was found that parallel finger configurations lead to poorer grasp performance even with soft adaptation when the grasp angle is not optimized for target objects, especially those with large aspect ratios such as pringles can and spatula in the YCB dataset [38]. Rearranging the soft fingers in a radial configuration leads to a more robust grasp [43], and a significant portion of existing commercial grippers are designed with two fingers in parallel. Hence, it is worthwhile to incorporate tactile sensing for a more robust parallel grasp. The objects used for the demonstration are aspect ratios between 2 to 4 and various weights.

While approaching the initial grasping pose, the SeeThruFinger detects if it has contact with the object by inferring real-time tactile feedback in 6D forces and torques based on the finger’s whole-body deformation. Due to the network design, the finger can deform twistedly to generate torque about the z -axis. When τ_z is detected to be larger than 0.05 Nm, the object orientation is severely different from the gripper’s initial pose, suggesting a less ideal grasping that can be optimized through regrasping by turning the wrist joint reversely to reduce τ_z for an enhanced adaptation and grasping robustness. When τ_z is within the threshold, the gripper closes its fingers until the gripping force f_x reaches the predefined maximum gripping force of 3 N. Then, the gripper lifts the object and drops it into the placing box. We repeated the process until all the five objects were cleared from the table.

Figure 11A shows the recorded 6D FT sensing data using the SeeThruFinger for the table-cleaning task, where the six peaks in f_x indicate the grasping of the six test objects. The inpainted scene using SeeThruFinger is shown in Fig. 11B, where the occluded regions are inpainted with coherent details, and the objects’ overall contours are well reconstructed. Although some surface textures generated are blurry, they are sufficiently accurate to reflect their actual textures. Figure 11C shows object detection results based on the inpainted scene, showing bounding boxes for each detected object. The most exciting result is the regrasping of the Bosche electrical screwdriver shown in Fig. 11D. By inspecting the detailed FT history in Fig. 11A, we identified two regrasping attempts of the Bosche electrical screwdriver performed by the SeeThruFinger based on tactile sensing and adaptive grasping.

Figure 11E is an enlarged view of the region marked in a red dashed box, as shown in Fig. 11A. When the SeeThruFinger performed the first grasping attempt in Fig. 11E(i), the finger detected the τ_z greater than 0.05 Nm in the negative direction. Then, in Fig. 11E(ii), the first reactive grasping begins rotating the gripper about the z -axis to reduce τ_z . During the process, the screwdriver suddenly turns to another side and temporarily loses contact with the finger in Fig. 11E(iii), as both f_x and f_y dropped to 0 suddenly. In Fig. 11E(iv), the gripper keeps closing, attempting to detect contact with the screwdriver again to keep increasing τ_z for an enhanced grasping pose. Next, the SeeThruFinger detected contact with the screwdriver again in Fig. 11E(v), marking the starting point of the second reactive grasping attempt. The SeeThruFinger repeated the same procedure by performing the second reactive grasping in Fig. 11E(vi), rotating

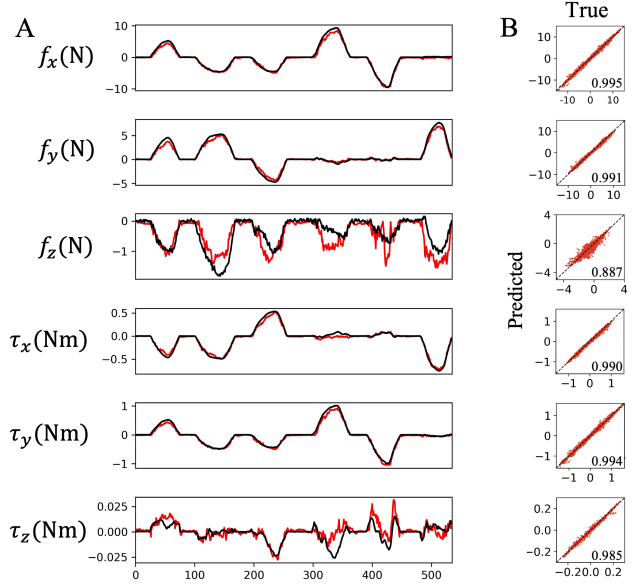


Figure 10: **Tactile sensing results using the Supervised Variational Autoencoder model via in-finger vision by tracking the SPN’s deformation masks.** (A) Test results for 6D forces and torques in sequence number, with the red lines as predicted and black lines as true measurements. (B) Quantitative comparison between the predicted values and true labels obtained from nano25.

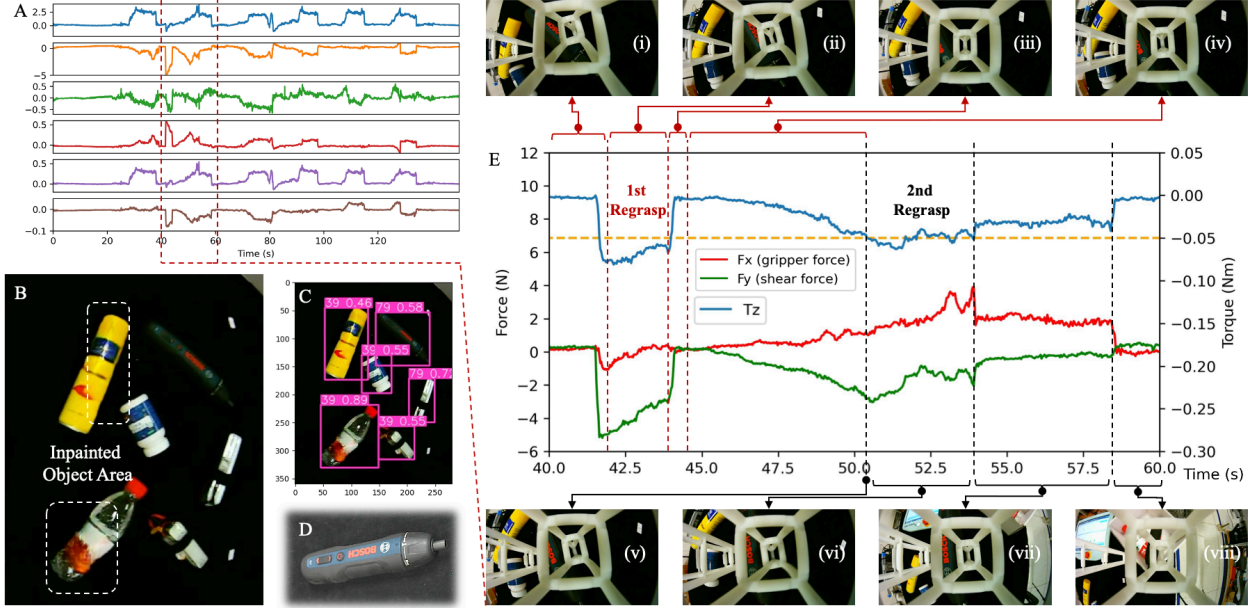


Figure 11: **SeeThruFinger demonstration results for reactive grasping task using SeeThruFingers.** (A) Inpainted scene via in-finger vision, where the white dashed boxes are inpainted portions of the scene and objects. (B) Visual perception of the in-painted scene via object detection. (C) The Bosche electrical screwdriver that requires reactive grasping. (D) Tactile sensing data was recorded in 6D forces and torques, where the red dashed box marks the reactive grasping process for the Bosche electrical screwdriver. (E) A detailed plot of the 6D forces and torques for the reactive grasping of the Bosche electrical screwdriver using the SeeThruFinger and multiple screenshots of in-finger vision.

the gripper about the z -axis until the detected τ_z is reduced towards 0. As a result, the screwdriver is secured between the fingers and moved toward the drop box in Fig. 11E(vii). Finally, the SeeThruFinger dropped the screwdriver with zero values detected from tactile sensing using in-finger vision, as shown in Fig. 11E(viii).

5 Towards a Multi-Modal Soft Touch

This section discusses the intuitive understanding of the three research problems illustrated in Fig. 6 regarding the SeeThruFinger (Fig. 1C) and the See-Thru-Network architecture (Fig. 3) towards multi-modal perception with a soft touch.

5.1 Markerless, Real-Time & Large-Scale Deformation Tracking of the See-Thru-Network

SeeThruFinger generically describes a class of soft robotic fingers/fingertips that involves a See-Thru-Network with in-finger vision as a design feature. The See-Through feature enables the in-finger vision to simultaneously capture visual features from the finger structure and the external environment. In this study, the See-Thru-Network is implemented using the Soft Polyhedral Networks. However, researchers have a wide range of design choices to customize the soft interface as needed, as long the resultant image contains sufficient details from both the finger structure and the external environment. The resultant performance is determined by the level of detail when extracting the soft structure's deformation and the reusable information left to reconstruct the scene.

Algorithmic development in video object segmentation is a well-researched field that enables convenient implementation of this capability for See-Thru-Networks with in-finger vision. The 30 Hz mask tracking implemented in this study is sufficiently high to enable real-time processing for robotics without adding to the computational burden of the robotic systems. Future research to allow a higher mask tracking bandwidth is preferred to increase the upper bound in collecting sensory feedback (towards 1,000 Hz) from in-finger vision, requiring higher framerate miniature cameras and high-performance mask tracking algorithms for more challenging robotic applications. The quality of mask segmentation at this step generally determines the maximum performance one can expect from the SeeThruFinger architecture in multi-modal perception. The solution to this problem provides the foundation to implement suitable robotic solutions for the second and third research problems involved in SeeThruFingers.

5.2 Multi-Modal Visual Perception of the Occluded Scene via In-Finger Vision

An intuitive understanding of the second research problem is whether we can use in-finger vision for environmental perception, which is multimodal by nature. This eliminates the need for an external camera in modern robot workstation setups.

Using in-finger vision for environmental perception is a counterintuitive application that can potentially remove the need for external cameras in a typical setup of robot workstations. Having an *Eye* camera fixed to the robot base is generally perceived as bio-inspired by humans or most living creatures, where visual organs are on the body for environmental perception, which is also shared by most robotic systems. After masked segmentation of the See-Thru-Network, the original image becomes fragmented. Still, it could be alternatively *repaired* using inpainting, a highly active field of research in computer vision and widely adopted practice throughout history. A direct result of inpainting the in-finger vision is the reconstruction of the scene, producing visual perceptual capabilities *almost* precisely as a typical Eye camera. It should be noted that the inpainting technique is computationally intensive, requiring high-performing hardware and long processing time, neither of which is ideal for robotic applications. In this study, we added an extra head-up motion during motion planning to collect an extra 1-second video clip for inpainting as a trade-off.

In the sections above, we demonstrated object detection using inpainted images from in-finger vision. Here, we showcase the performance of achieving other modalities, such as depth sensing and scene segmentation, using the inpainted images, which are also widely used in modern robotics. In principle, robotists can reuse the inpainted images for any desirable extra modalities as needed in the same way as a computer vision problem, making the SeeThruFinger architecture a generic solution for robotics where constraints in hardware cost and computational power are of significant consideration.

5.2.1 Depth Sensing

As a proof-of-concept, we conducted the monocular depth estimation based on the inpainted scene. We compared the reconstructed scene depths from both the in-finger camera and a camera with an unobstructed view of the robot’s working space. In this experiment, ten objects with various shapes and colors (milk powder can, tape, rubber ball, strawberry, glue, plum, glue stick, power drill with a packaging box, and drill toolkit) were placed on the tabletop. The robotic arm swept across the tabletop from left to right and returned to the starting point with a fixed orientation while the in-finger camera inspected the objects. We recorded both the in-finger and unobstructed videos by removing the SPN from the gripper. The former was further inpainted by E²FGVI algorithm. The inpainted and unobstructed videos are then fed to the Depth Anything V2 model [44] to obtain the depth estimations. The pixel-wise estimations are relative depth values, providing helpful information on the relative poses of the objects on the table. Hence, instead of comparing the actual values of the depth map, we adopt the structural similarity index (SSI) to evaluate the similarity between the depth map reconstructed from the inpainted view and that from the unobstructed view.

As shown in Fig. 12A, the index varies between 0.71 and 0.95 with an average of 0.87. Figure 12B-D shows three snapshots of in-finger vision, the depth map estimated from the inpainted view, and the SSI map. Low SSI values prominently occur at the objects’ edges, where depth estimation is inherently more challenging.

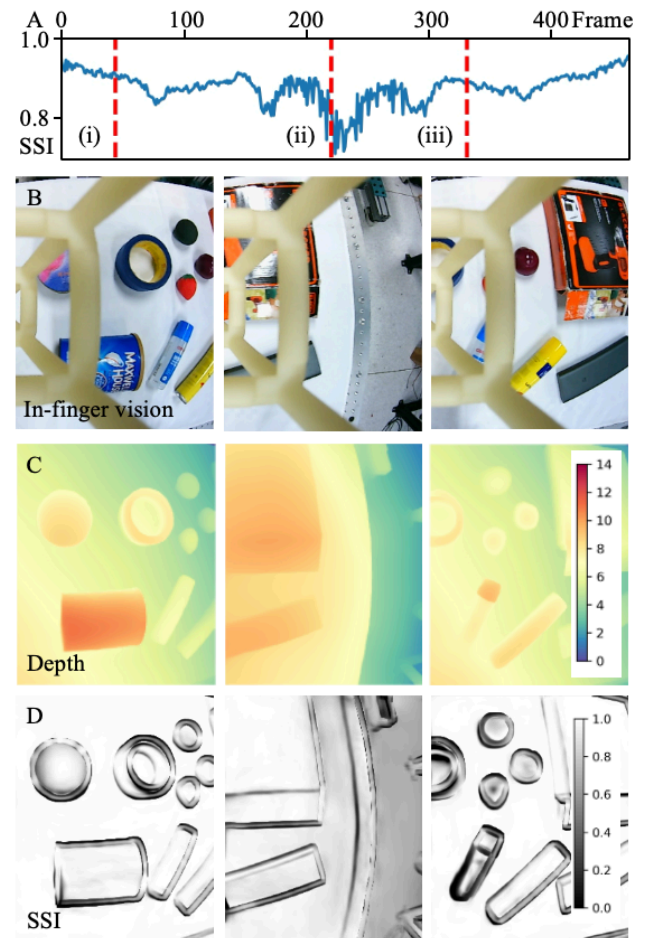


Figure 12: **Depth estimation by seeing through the finger after inpainting.** (A) Time series of Structural similarity index (SSI) measures between depth estimations from the inpainted and unobstructed views. The red lines marked in (i), (ii), and (iii) indicate the snapshot frames of (B) in-finger vision, (C) reconstructed depth map, and (D) SSI map. See the supplementary video for further demonstration.

5.2.2 Scene Segmentation

Furthermore, we explored the feasibility of multi-object segmentation on the inpainted scene using the latest Segment Anything Model 2 (SAM 2) [45]. We tested on the same scene described in the depth estimation task. As shown in Fig. 13A, segmentation on the inpainted view achieves satisfactory performance with J measurement ranging between 0.64 and 0.87, which is 16% lower than the performance of segmentation on the unobstructed view on average. An interesting observation occurred in the segmentation of object 9 (a power drill with a packaging box), where the inpainted view performed better than the unobstructed view. Further frame-by-frame examination shows that the worse segmentation in the unobstructed view was caused by the intense surface reflection of the drill’s packaging box, and in some frames, SAM2 failed to segment object 9. On the contrary, SAM2 kept tracking object nine well in the inpainted view (see supplementary video). The snapshots of the unobstructed and in-finger vision and segmentations of the inpainted scene at two different times are shown in Figs. 13C&D.

5.3 Multi-Modal & Markerless Vision-based Tactile Sensing with the SeeThruFinger

An intuitive understanding of the third research problem is whether we can use in-finger vision with the SeeThruFingers to achieve high-performing, multi-modal tactile sensing in a markerless way. Similar capabilities have been widely researched in the past literature, but the involvement of artificial markers remains a challenge among the current solutions [46, 32, 47, 48]. In this study, a by-product while addressing the first research problem is the real-time, pixel-wise segmentation of the See-Thru-Network’s mask M_t^{Seg} throughout the implementation of the SeeThruFinger architecture. Visual features from this mask provide a robust sensory input to infer force-and-torque information for tactile grasping once a calibration dataset is obtained against commercial force-and-torque sensors for model training.

While it is reasonable to use simpler neural networks, we adopted a generative approach in this study and utilized the Supervised Variational Autoencoder (SVAE) to address this problem. The latent variables obtained from SVAE are a powerful tool to infer various sensory modalities, requiring little disruption to the overall computational architecture. Besides the 6D force-and-torque, we demonstrate a simple implementation to infer the contact event on the SeeThruFinger. Recent research also shows promising results in proprioceptive shape reconstruction, contact point estimation, and tactile sensing using in-finger vision with the soft polyhedral networks used in this study, which could be further implemented using the deformation mask tracked in this study.

5.3.1 Contact Event Detection

In previous work where the complex deformations of SPN are physically encoded into a much lower 6D space of Aruco Marker pose, the contact location information has been lost [33]. With a much higher dimension of 32 in the SVAE framework, We hypothesize such information could be maintained in the latent space to a certain degree.

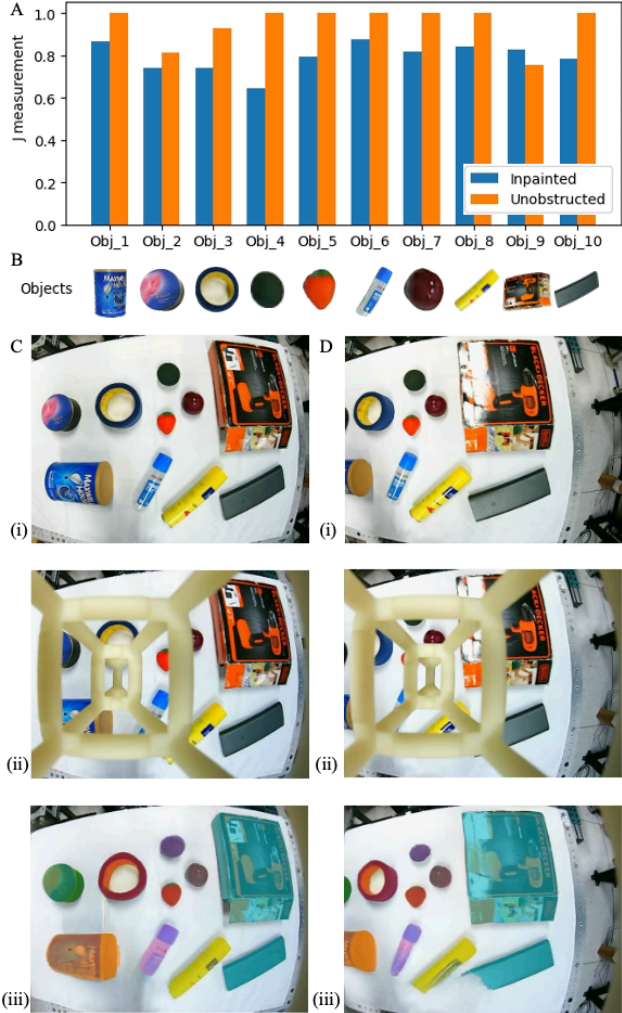


Figure 13: **Segmentation by seeing through the finger.** (A) The performance comparison of SAM2 on the inpainted and the unobstructed view of ten objects, measured by intersection over Union (Jaccard index); (B) Ten objects with various shapes and colors: milk powder can, tape, rubber ball, strawberry, glue, plum, glue stick, power drill with a packaging box, and drill toolkit; (C) Snapshot of the unobstructed and in-finger vision and the resultant segmentation of the inpainted scene; (D) A different snapshot similar to (C). See the supplementary video for further demonstration.

A preliminary test was conducted by categorizing the training samples into three contact events: no contact, contact at the finger’s tip, and middle regions. We trained a contact event classifier using the SVAE framework shown in Fig. 9, which can be formulated by

$$\{\mathbf{Event}_{\text{Contact}}, \mathbf{M}^{\text{Gen}}\} = f_3(\text{Dynamic}^{\text{STN}}\mathbf{M}^{\text{Seg}}, \mathbf{M}_{t=0}^{\text{Seg}}), \quad (5)$$

$$f_3 = \text{SVAE}.$$

Figure 14 shows the confusion matrix of the classifier evaluated on the validation dataset of 8000 samples. The accuracies for all three contact events are above 97%. Considering the classifier only takes the SPN’s mask as input, which filters out all the see-through visual information, the results confirm our hypothesis that the soft touch represented by the latent vectors contains tactile details such as resultant force/torque and contact location. A real-time demonstration is included in the video supplementary. The binary classes of the contact location are partly limited by the data collection process, where the precise locations were not recorded. The granularity might be further improved by having more dense labels or even becoming a regression task.

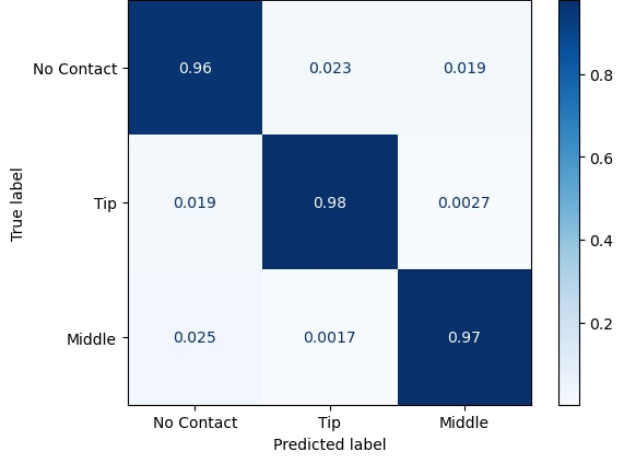


Figure 14: **Confusion matrix of contact event detection.** The tip and middle labels refer to the top and middle regions of the soft polyhedral network during contact. See the supplementary video for further demonstration.

5.4 Multi-Modal Perceptual Embodiment via a Soft Touch

Using a single sensory input from the in-finger vision of a SeeThruFinger featuring See-Thru-Networks, this study presents a multi-modal approach towards robotic perceptual embodiment via vision-based tactile sensing with a soft touch, as shown in Fig. 15. Our proposed SeeThruFinger architecture generates various outputs for extrinsic perception, including inpainted scenes, object detection, depth sensing, and scene segmentation. For intrinsic perceptions, we have demonstrated the implementation of the SeeThruFinger architecture that generates outputs including masked deformation tracking, 6D force and torque sensing in real-time and high accuracy, and contact event detection. Further expansion to other intrinsic or extrinsic modalities can be implemented depending on the specific need in robotics or applications.

6 Conclusion & Future Works

This paper presents the SeeThruFinger architecture for Multi-Modal and Vision-Based Tactile Sensing via a See-Thru-Network, simultaneously achieving multi-modal visual perception and tactile sensing through a single in-finger vision of the Soft Polyhedral Networks. The occluded in-finger vision provides sufficient scene details that could be algorithmically inpainted for visual perception. This is achieved by tracking a deformable mask of the Soft Polyhedral Network during contact-based interactions using real-time video object segmentation. The omni-directional adaptation of the Soft Polyhedral Network provides a rich set of visual features that could be directly used to learn a tactile sensing model for reactive grasping. Using masked Soft Polyhedral Networks as the visual input effectively removes the necessity for artificial markers in vision-based tactile sensing. The resultant SeeThruFinger architecture enables multi-modal perception of the scene, including globalized scene segmentation object detection and localized tactile sensing at high accuracy. As reported in this study, a direct benefit is the possibility of completely removing the external camera while simultaneously providing physical compliance, visual perception, and tactile sensing using just one in-finger vision. Our proposed SeeThruFinger architecture should also apply to other vision-based tactile sensing solutions with an illuminated chamber by removing the opaque coating on the outer surface of the soft membrane [28]. However, the performance may be reduced due to the blurry image of the scene occluded by the transparent soft membrane, which may only work at a very close range that is insufficient for visual perception of the whole scene [49].

Our work has several limitations. Even though the XMem is reasonably fast (30 Hz), it is still far from the chosen camera’s 330 Hz framerate. The whole pipeline is not as efficient yet, which requires further optimization for robotic interactions. In this work, we did not fine-tune the object detection model for the objects tested, and the object detection results show mislabeled object classes even though they can be detected. The learned tactile perception model is subject to a systematic shift when applied to a new finger that is not presented in the training dataset due to the slight difference

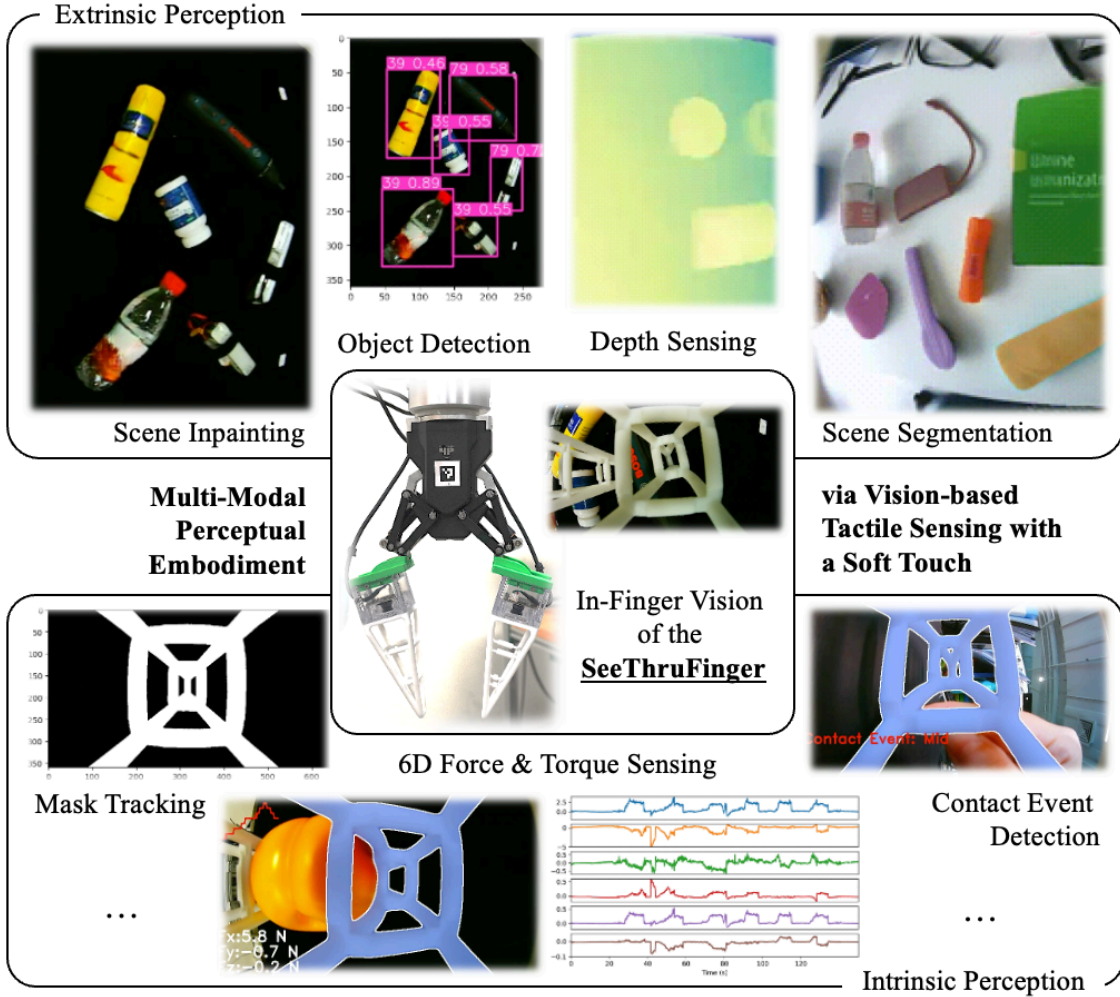


Figure 15: Towards Multi-Modal Perceptual Embodiment via Vision-based Tactile Sensing with the SeeThruFinger architecture, which generates multiple modalities of intrinsic and extrinsic perception simultaneously based on a single input from the SeeThruFinger’s in-finger vision.

in the initial template mask of each finger. Although we fed the initial template mask along with the instantaneous one, SVAE failed to encode the geometric deformation compared to the template mask, probably because it only saw two templates during training. Besides mitigating this systematic error by simple subtraction, a promising way is through data augmentation.

There are a few directions we would like to explore further in the future. One is underwater visual perception and tactile sensing using SeeThruFinger by translating models learned on land to underwater scenarios, aiming at dexterous and sensitive exploration underwater [50]. Due to the unique design, the SeeThruFinger can be directly used underwater if the camera housing is waterproofed [36], which is quite simple as there are no dynamic seals. Another potential application is embodied robot learning with multi-modal tactile perception, where the SeeThruFingers can be a promising solution to introduce simultaneous benefits in omni-directional adaptation in grasping while providing a rich set of perceptual modalities including high-performing 6D force-and-torque sensing, which are yet to be implemented with ease for systems such as the Universal Manipulation Interface [51]. In this study, only one of the SeeThruFingers’ in-finger vision was used, but both are fully functional. It would be interesting to see if the stereo vision for 3D reconstruction or 6D pose estimation based on the inpainted scene from both in-finger visions would be possible. This is another exciting direction we would like to explore further.

Acknowledgement

This work was partly supported by the National Natural Science Foundation of China under Grant 62206119 and Grant 62473189, the Science, Technology, and Innovation Commission of Shenzhen Municipality under Grant JCYJ20220818100417038, Shenzhen Long-Term Support for Higher Education at SUSTech under Grant 20231115141649002 and SUSTech Virtual Teaching Lab for Machine Intelligence Design and Learning under Grant XJZLGC202241.

Author Fang Wan would like to thank Prof. Roberto Calandra and all organizers and participants of the 2024 Touch Sensing and Processing Summer School in Dresden for their valuable discussions and constructive feedback on this work.

Supplementary Materials

Please refer to this link for a supplementary video of this paper.

References

- [1] Niko Sünderhauf, Oliver Brock, Walter Scheirer, Raia Hadsell, Dieter Fox, Jürgen Leitner, Ben Upcroft, Pieter Abbeel, Wolfram Burgard, Michael Milford, and Peter Corke. The Limits and Potentials of Deep Learning for Robotics. *The International Journal of Robotics Research*, 37(4-5):405–420, 2018.
- [2] Yann LeCun, Yoshua Bengio, and Geoffrey Hinton. Deep Learning. *Nature*, 521(7553):436–444, 2015.
- [3] Peter Meer, Doron Mintz, Azriel Rosenfeld, and Dong Yoon Kim. Robust Regression Methods for Computer Vision: A Review. *International Journal of Computer Vision*, 6:59–70, 1991.
- [4] Alexander Kirillov, Eric Mintun, Nikhila Ravi, Hanzi Mao, Chloe Rolland, Laura Gustafson, Tete Xiao, Spencer Whitehead, Alexander C. Berg, Wan-Yen Lo, Piotr Dollár, and Ross Girshick. Segment Anything. In *arXiv:2304.02643 [cs.CV]*, 2023.
- [5] Ho Kei Cheng and Alexander G Schwing. XMem: Long-Term Video Object Segmentation with an Atkinson-Shiffrin Memory Model. In *European Conference on Computer Vision (ECCV)*, 2022.
- [6] Gao Huang, Zhuang Liu, Laurens Van Der Maaten, and Kilian Q Weinberger. Densely Connected Convolutional Networks. In *IEEE Conference on Computer Vision and Pattern Recognition (CVPR)*, pages 4700–4708, 2017.
- [7] Erik Murphy-Chutorian and Mohan Manubhai Trivedi. Head Pose Estimation in Computer Vision: A Survey. *IEEE Transactions on Pattern Analysis and Machine Intelligence*, 31(4):607–626, 2008.
- [8] Tao Yu, Runseng Feng, Ruoyu Feng, Jinming Liu, Xin Jin, Wenjun Zeng, and Zhibo Chen. Inpaint Anything: Segment Anything Meets Image Inpainting. In *arXiv:2304.06790 [cs.CV]*, 2023.
- [9] Ben Mildenhall, Pratul P Srinivasan, Matthew Tancik, Jonathan T Barron, Ravi Ramamoorthi, and Ren Ng. NeRF: Representing Scenes as Neural Radiance Fields for View Synthesis. *Communications of the ACM*, 65(1):99–106, 2021.
- [10] David Howard, Agoston E. Eiben, Danielle Frances Kennedy, Jean-Baptiste Mouret, Philip Valencia, and Dave Winkler. Evolving Embodied Intelligence from Materials to Machines. *Nature Machine Intelligence*, 1(1):12–19, 2019.
- [11] Oliver Kroemer, Scott Niekum, and George Konidaris. A Review of Robot Learning for Manipulation: Challenges, Representations, and Algorithms. *Journal of Machine Learning Research*, 22(30):1–82, 2021.
- [12] OpenAI, Ilge Akkaya, Marcin Andrychowicz, Maciek Chociej, Mateusz Litwin, Bob McGrew, Arthur Petron, Alex Paino, Matthias Plappert, Glenn Powell, Raphael Ribas, Jonas Schneider, Nikolas A. Tezak, Jerry Tworek, Peter Welinder, Lilian Weng, Qiming Yuan, Wojciech Zaremba, and Lei M. Zhang. Solving Rubik’s Cube with a Robot Hand. In *arXiv:1910.07113 [cs.LG]*, 2019.
- [13] Su-Fang Zhang, Jun-Hai Zhai, Bo-Jun Xie, Yan Zhan, and Xin Wang. Multimodal Representation Learning: Advances, Trends and Challenges. In *2019 International Conference on Machine Learning and Cybernetics (ICMLC)*, pages 1–6, 2019.
- [14] Fang Wan, Haokun Wang, Xiaobo Liu, Linhan Yang, and Chaoyang Song. DeepClaw: A Robotic Hardware Benchmarking Platform for Learning Object Manipulation. In *IEEE/ASME International Conference on Advanced Intelligent Mechatronics (AIM)*, pages 2011–2018, 2020.

- [15] Bojun Ouyang and Dan Raviv. Occlusion Guided Scene Flow Estimation on 3D Point Clouds. In *IEEE/CVF Conference on Computer Vision and Pattern Recognition Workshops (CVPRW)*, pages 2799–2808, 2021.
- [16] Federico Angelini, Zeyu Fu, Yang Long, Ling Shao, and Syed Mohsen Naqvi. 2D Pose-Based Real-Time Human Action Recognition With Occlusion-Handling. *IEEE Transactions on Multimedia*, 22(6):1433–1446, 2020.
- [17] Tobia Marcucci, Mark Petersen, David von Wrangel, and Russ Tedrake. Motion Planning around Obstacles with Convex Optimization. *Science Robotics*, 8(84):eadf7843, 2023.
- [18] Hao Tian, Chaoyang Song, Changbo Wang, Xinyu Zhang, and Jia Pan. Sampling-Based Planning for Retrieving Near-Cylindrical Objects in Cluttered Scenes Using Hierarchical Graphs. *IEEE Transactions on Robotics*, 39(1):165–182, 2023.
- [19] E. Macaluso and A. Maravita. The Representation of Space Near the Body through Touch and Vision. *Neuropsychologia*, 48(3):782–795, 2010.
- [20] Michelle Lee, Yuke Zhu, Peter Zachares, Matthew Tan, Krishnan Srinivasan, Silvio Savarese, Li Fei-Fei, Animesh Garg, and Jeannette Bohg. Making Sense of Vision and Touch: Learning Multimodal Representations for Contact-Rich Tasks. *IEEE Transactions on Robotics*, PP:1–15, 03 2020.
- [21] S. Begej. Planar and Finger-shaped Optical Tactile Sensors for Robotic Applications. *IEEE Journal on Robotics and Automation*, 4(5):472–484, 1988.
- [22] Kazuhiro Shimonomura. Tactile Image Sensors Employing Camera: A Review. *Sensors*, 19:3933, 09 2019.
- [23] Yue Liu, Rongrong Bao, Juan Tao, Jing Li, Ming Dong, and Caofeng Pan. Recent Progress in Tactile Sensors and Their Applications in Intelligent Systems. *Science Bulletin*, 65(1):70–88, 2020.
- [24] Benjamin Shih, Dylan Shah, Jinxing Li, Thomas G. Thuruthel, Yong-Lae Park, Fumiya Iida, Zhenan Bao, Rebecca Kramer-Bottiglio, and Michael T. Tolley. Electronic Skins and Machine Learning for Intelligent Soft Robots. *Science Robotics*, 5(41):eaaz9239, 2020.
- [25] Qiang Li, Oliver Kroemer, Zhe Su, Filipe Fernandes Veiga, Mohsen Kaboli, and Helge Joachim Ritter. A Review of Tactile Information: Perception and Action Through Touch. *IEEE Transactions on Robotics*, 36(6):1619–1634, 2020.
- [26] Shixin Zhang, Zixi Chen, Yuan Gao, Weiwei Wan, Jianhua Shan, Hongxiang Xue, Fuchun Sun, Yiyong Yang, and Bin Fang. Hardware Technology of Vision-Based Tactile Sensor: A Review. *IEEE Sensors Journal*, 22(22):21410–21427, 2022.
- [27] Vijay Kakani, Xuenan Cui, Mingjie Ma, and Hakil Kim. Vision-Based Tactile Sensor Mechanism for the Estimation of Contact Position and Force Distribution Using Deep Learning. *Sensors*, 21(5), 2021.
- [28] Wenzhen Yuan, Siyuan Dong, and Edward H. Adelson. GelSight: High-Resolution Robot Tactile Sensors for Estimating Geometry and Force. *Sensors*, 17(12), 2017.
- [29] Carmelo Sferrazza and Raffaello D’Andrea. Design, Motivation and Evaluation of a Full-Resolution Optical Tactile Sensor. *Sensors*, 19(4), 2019.
- [30] Jialiang Zhao and Edward H. Adelson. GelSight Svelte: A Human Finger-Shaped Single-Camera Tactile Robot Finger with Large Sensing Coverage and Proprioceptive Sensing. In *IEEE/RSJ International Conference on Intelligent Robots and Systems (IROS)*, pages 8979–8984, 2023.
- [31] Akihiko Yamaguchi and Christopher G. Atkeson. Implementing Tactile Behaviors using FingerVision. In *IEEE-RAS 17th International Conference on Humanoid Robotics (Humanoids)*, pages 241–248, 2017.
- [32] Mike Lambeta, Po-Wei Chou, Stephen Tian, Brian Yang, Benjamin Maloon, Victoria Rose Most, Dave Stroud, Raymond Santos, Ahmad Byagowi, Gregg Kammerer, Dinesh Jayaraman, and Roberto Calandra. DIGIT: A Novel Design for a Low-Cost Compact High-Resolution Tactile Sensor With Application to In-Hand Manipulation. *IEEE Robotics and Automation Letters*, 5(3):3838–3845, 2020.
- [33] Xiaobo Liu, Xudong Han, Wei Hong, Fang Wan, and Chaoyang Song. Proprioceptive Learning with Soft Polyhedral Networks. *The International Journal of Robotics Research*, 0(0):02783649241238765, 2024.
- [34] Fang Wan, Xiaobo Liu, Ning Guo, Xudong Han, Feng Tian, and Chaoyang Song. Visual Learning towards Soft Robot Force Control using a 3D Metamaterial with Differential Stiffness. In Aleksandra Faust, David Hsu, and Gerhard Neumann, editors, *Proceedings of the 5th Conference on Robot Learning*, volume 164 of *Proceedings of Machine Learning Research*, pages 1269–1278. PMLR, 08–11 Nov 2022.
- [35] Ning Guo, Xudong Han, Shuqiao Zhong, Zhiyuan Zhou, Jian Lin, Fang Wan, and Chaoyang Song. Reconstructing Soft Robotic Touch via In-Finger Vision. *Advanced Intelligent Systems*, 6(10):2400022, 2024.

- [36] Ning Guo, Xudong Han, Shuqiao Zhong, Zhiyuan Zhou, Jian Lin, Jiansheng Dai, Fang Wan, and Chaoyang Song. Proprioceptive State Estimation for Amphibious Tactile Sensing. *IEEE Transactions on Robotics*, 2024.
- [37] Ning Guo, Xudong Han, Xiaobo Liu, Shuqiao Zhong, Zhiyuan Zhou, Jian Lin, Jiansheng Dai, Fang Wan, and Chaoyang Song. Autoencoding a Soft Touch to Learn Grasping from On-Land to Underwater. *Advanced Intelligent Systems*, 6(1):2300382, 2024.
- [38] Berk Calli, Arjun Singh, Aaron Walsman, Siddhartha Srinivasa, Pieter Abbeel, and Aaron M. Dollar. The YCB Object and Model set: Towards Common Benchmarks for Manipulation Research. In *International Conference on Advanced Robotics (ICAR)*, pages 510–517, 2015.
- [39] F. Perazzi, J. Pont-Tuset, B. McWilliams, L. Van Gool, M. Gross, and A. Sorkine-Hornung. A Benchmark Dataset and Evaluation Methodology for Video Object Segmentation. In *2016 IEEE Conference on Computer Vision and Pattern Recognition (CVPR)*, pages 724–732, 2016.
- [40] Weize Quan, Jiayi Chen, Yanli Liu, Dong-Ming Yan, and Peter Wonka. Deep Learning-Based Image and Video Inpainting: A Survey. *International Journal of Computer Vision*, 132(7):2367–2400, 2024.
- [41] Zhen Li, Cheng-Ze Lu, Jianhua Qin, Chun-Le Guo, and Ming-Ming Cheng. Towards An End-to-End Framework for Flow-Guided Video Inpainting. In *IEEE/CVF Conference on Computer Vision and Pattern Recognition (CVPR)*, pages 17541–17550, 2022.
- [42] Yian Zhao, Wenyu Lv, Shangliang Xu, Jinman Wei, Guanzhong Wang, Qingqing Dang, Yi Liu, and Jie Chen. DETRs Beat YOLOs on Real-time Object Detection. In *IEEE/CVF Conference on Computer Vision and Pattern Recognition (CVPR)*, pages 16965–16974, 2024.
- [43] Fang Wan, Haokun Wang, Jiayuan Wu, Yujia Liu, Sheng Ge, and Chaoyang Song. A Reconfigurable Design for Omni-Adaptive Grasp Learning. *IEEE Robotics and Automation Letters*, 5(3):4210–4217, 2020.
- [44] Lihe Yang, Bingyi Kang, Zilong Huang, Zhen Zhao, Xiaogang Xu, Jiashi Feng, and Hengshuang Zhao. Depth Anything V2. In *arXiv:2406.09414 [cs.CV]*, 2024.
- [45] Nikhila Ravi, Valentin Gabeur, Yuan-Ting Hu, Ronghang Hu, Chaitanya Ryali, Tengyu Ma, Haitham Khedr, Roman Rädle, Chloe Rolland, Laura Gustafson, Eric Mintun, Junting Pan, Kalyan Vasudev Alwala, Nicolas Carion, Chao-Yuan Wu, Ross Girshick, Piotr Dollár, and Christoph Feichtenhofer. SAM 2: Segment Anything in Images and Videos. In *arXiv:2408.00714 [cs.CV]*, 2024.
- [46] Akihiko Yamaguchi and Christopher G. Atkeson. Combining Finger Vision and Optical Tactile Sensing: Reducing and Handling Errors while Cutting Vegetables. In *2016 IEEE-RAS 16th International Conference on Humanoid Robots (Humanoids)*, pages 1045–1051, 2016.
- [47] Nathan F. Lepora. Soft Biomimetic Optical Tactile Sensing With the TacTip: A Review. *IEEE Sensors Journal*, 21(19):21131–21143, 2021.
- [48] Wen Fan, Haoran Li, Weiyong Si, Shan Luo, Nathan Lepora, and Dandan Zhang. ViTacTip: Design and Verification of a Novel Biomimetic Physical Vision-Tactile Fusion Sensor, 2024.
- [49] Francois R. Hogan, Jean-François Tremblay, Bobak H. Baghi, Michael Jenkin, Kaleem Siddiqi, and Gregory Dudek. Finger-STs: Combined Proximity and Tactile Sensing for Robotic Manipulation. *IEEE Robotics and Automation Letters*, 7(4):10865–10872, 2022.
- [50] Oussama Khatib, Xiyang Yeh, Gerald Brantner, Brian Soe, Boyeon Kim, Shameek Ganguly, Hannah Stuart, Shiquan Wang, Mark Cutkosky, Aaron Edsinger, Phillip Mullins, Mitchell Barham, Christian R. Woolstra, Khaled Nabil Salama, Michel L’Hour, and Vincent Creuze. Ocean One: A Robotic Avatar for Oceanic Discovery. *IEEE Robotics and Automation Magazine*, 23(4):20–29, 2016.
- [51] Cheng Chi, Zhenjia Xu, Chuer Pan, Eric Cousineau, Benjamin Burchfiel, Siyuan Feng, Russ Tedrake, and Shuran Song. Universal Manipulation Interface: In-The-Wild Robot Teaching Without In-The-Wild Robots. In *Proceedings of Robotics: Science and Systems (RSS)*, 2024.